Supplement of Atmos. Chem. Phys., 15, 11011–11026, 2015
http://www.atmos-chem-phys.net/15/11011/2015/
doi:10.5194/acp-15-11011-2015-supplement

Atmospheric Chemistry and Physics Open Access

Supplement of

Black carbon, particle number concentration and nitrogen oxide emission factors of random in-use vehicles measured with the on-road chasing method

I. Ježek et al.

Correspondence to: I. Ježek (irena.jezek@aerosol.si) and G. Močnik (grisa.mocnik@aerosol.si)

Supplementary material S1 – BC, NOx and PN formation in combustion engines

NO_x and BC do not have the same formation process in the engine: while NO_x is formed in fuel lean conditions and at high temperatures, BC is formed in fuel rich conditions. Most of the NO_x in the engine is formed by the Zeldovich mechanism, where NO is formed from atmospheric nitrogen (and its destruction) (Heywood, 1988). Soot (or BC) formation does not have as clear a formation path. According to Xi and Zhong, 2006, the soot formation steps can be summarized as the: "(1) formation of molecular precursors of soot, (2) nucleation or inception of particles from heavy polycyclic aromatic hydrocarbon molecules, (3) mass growth of particles through the addition of gas phase molecules, (4) coagulation via reactive particle-particle collisions, (5) carbonization of particulate material, and, finally, (6) oxidation of polycyclic aromatic hydrocarbons and soot particles".

In gasoline engines, the fuel and air are mixed before they are injected in the combustion chamber: the mix is homogenous and the engine can smoothly operate close to stoichiometric or slightly fuel-rich mixture. In fuel rich conditions, hydrocarbon (HC) and carbon monoxide (CO) formation is high, and soot emissions can also occur; in lean to stoichiometric conditions, NO formation increases. Because engines operate in different modes, several (and different) emission control techniques are necessary to reduce all pollutants. The reason diesel engines emit more soot and NO than gasoline engines is because in diesel engines the fuel is injected in the chamber just before the combustion starts. The fuel-to-air ratio in the mixture and the combustion temperature are not homogenous, leading to higher NO formation in the close to-stoichiometric regions and to soot formation in the rich unburned-fuel containing core of the fuel spray. The majority of soot particles thus formed, can then oxidize in the presence of unburned oxygen (Heywood, 1988).

In diesel vehicles, high soot emissions occur when the relative air-fuel ratio drops to very low values during the early cycles of a transient event, when the air supply by the compressor cannot meet the higher fuel flow during load increase; since the fuel pump responds much faster than the air supply, the combustion efficiency deteriorates and leads to a slow engine (torque and speed) response and an overshoot in particulate, gaseous, and noise emissions. There are various delays that affect the transient engine response; in wide spread turbocharged diesel engines, the poor load acceptance is even worse than in naturally aspired engines because of the flow and the dynamic inertia of the turbocharger (Tavčar et al., 2011, and references therein).

Particles emitted from the vehicle exhaust consist mainly of highly agglomerated solid carbonaceous material, ash and volatile organic and Sulphur compounds (Kittelson, 1998). Carbonaceous soot particles are formed in the combustion process and are mostly found in the accumulation mode; at the tailpipe where the exhaust dilutes and cools the volatile precursors may nucleate or adsorb on pre-existing particles (Kittelson et al., 2006). The composition of the exhaust particles changes under different vehicle load conditions (Ježek et al., 2015; Kittelson, 1998; Sharma et al., 2005). Unlike particle mass (PM), particle number (PN) concentration is not conserved in the atmosphere (Kittelson, 1998). The particle number and size distribution strongly depend on dilution and sampling conditions; the gas to particle conversion processes, nucleation, condensation and adsorption are non-linear and extremely sensitive to conditions, thus the on-road emissions are not easy to reproduce in laboratory (Kittelson et al., 2006). In the atmosphere the residence time for particles in diameter range 0.1-10 μm is about a week and for 10 nm particles about 15 minutes (Harrison et al., 1996). In this time smaller particles coagulate with larger ones, thus losing their identity as individual particles but ultimately remaining in the atmosphere for the same amount of time (Harrison et al., 1996, Kittelson, 1998). Smaller particles – in ultrafine and nanoparticle diameter range, may be more health hazardous as they can penetrate deeper in to lungs and eventually in the blood system (Dockery et al., 1993; Kennedy, 2007). With the newest vehicle emission standard Euro 6 (European Parliment, 2007) also PN emission standards for both gasoline and diesel cars came in to force.

Figure S1. Photographs from the on-road measurement campaign. The image on the top left is the background measurement, the top right is the beginning of a chase of a truck with a trailer; the lower image depicts a car chase.

Supplementary material S2 – additional Eurostat data information

European countries that reported passenger cars fleet composition for year 2011 were: Belgium, Czech Republic, Germany, Estonia, Ireland, Spain, Croatia, Italy, Cyprus, Latvia, Lithuania, Hungary, Malta, Netherlands, Poland, Portugal, Romania, Slovenia, Finland, Sweden, United Kingdom, Norway, Switzerland, Former Yugoslav Republic of Macedonia, and Turkey

Unfortunately this type of Eurostat data was not available for France, which has the third largest segment (13.3%) of Europe's car fleet (according to Eurostat data for 2010). However, the ACEA (European Car Manufacturers' Association) reported a similar percentage of diesel and gasoline cars in the European fleet in their 2012 pocket guide (ACEA, 2012); they included the following countries: Austria, Belgium, Czech Republic, Denmark, Finland, France, Germany, Greece, Italy, Latvia, Lithuania, Netherlands, Poland, Romania, Spain, Sweden and the UK; they report 61.5% of vehicles using gasoline, 35.3% using diesel and 3.2% using other fuel types. The portion of diesel passenger cars in Europe is therefore around 35%.

Countries that reported lorries fleet composition: Malta, Latvia, Estonia, Cyprus, Slovenia, Croatia, Lithuania, Romania, Finland, Czech Republic, Ireland, Switzerland, Norway, Portugal, Netherlands, Sweden, Italy, Spain and Germany. Some countries reported different total numbers of their lorries regarding the age and size segregation. We kept most but excluded Poland because the difference between the two was over two million.

Supplementary material S3 – additional uncertainty analysis

In order to investigate the effect of exhaust dilution on the determination of the EF by chasing, and to further explain the results of the running integration calculation, we evaluated the chasing method using tailpipe measurements of CO_2 by PEMS. In this test we wanted to see how mobile measurements match the direct in-exhaust measurements of the chased vehicle. From these measurements we calculated the dilution rate (DR) as a ratio of the CO_2 measured by PEMS and by the chasing instrument (Chang et al., 2009), and compared it to the calculated BC EF.

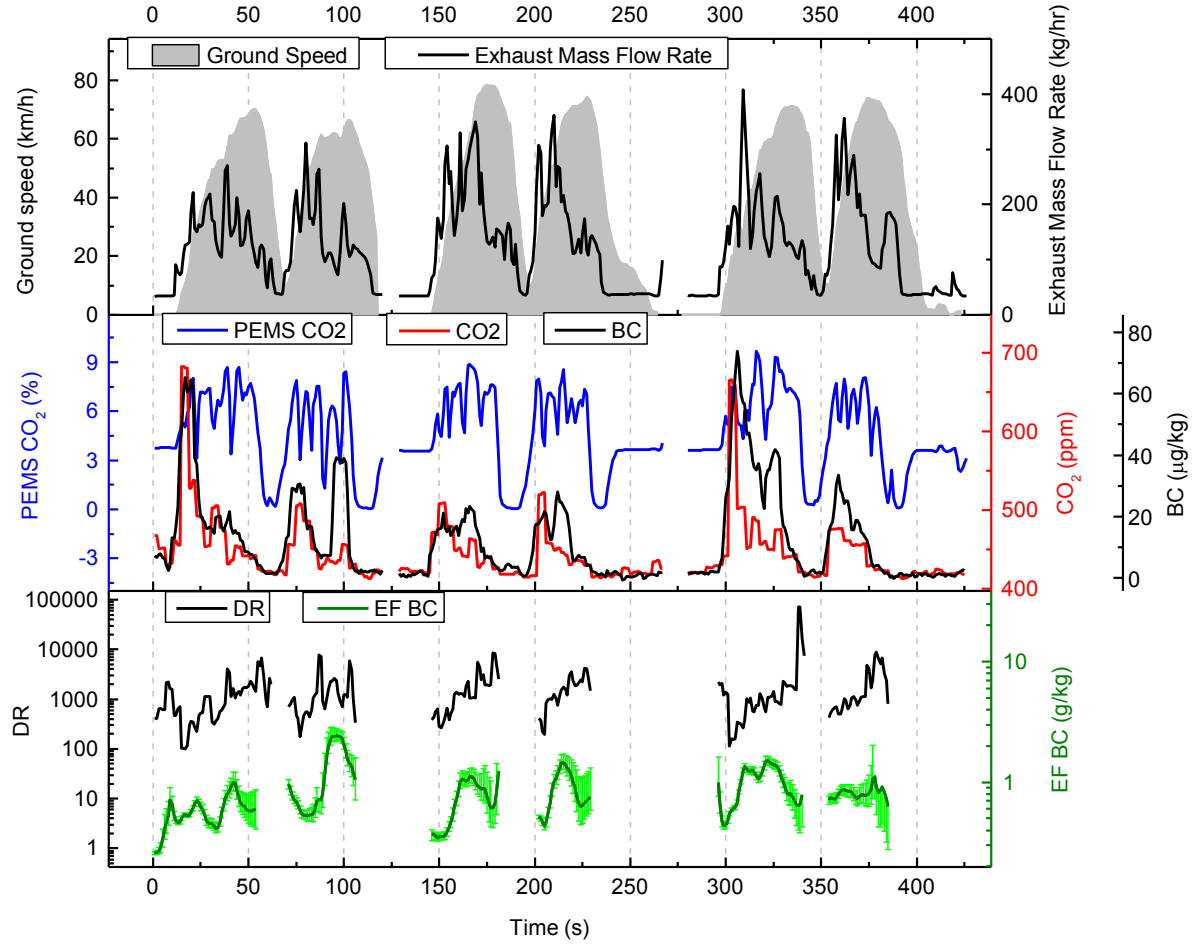

Figure S2. The tailpipe measurements performed with the portable emission measurement system (PEMS) are ground speed (shaded grey) and exhaust mass flow rate (black) – top; and CO_2 (blue) – middle. CO_2 and BC measured with the mobile station in red and black, respectively, also in the middle plot. The calculated dilution ratio (DR) in black and the BC EF in green – bottom. The BC EF does not show any significant dependence on the DR, and the uncertainty of EF (light green) increases when the CO_2 emissions are low. Note the log scales for DR and EF. Data from Ježek et al., 2015.

The results presented in Figure S2 first show how the exhaust mass flow rate changes with the vehicle speed for the analyzed turbocharged diesel engine. When the vehicle is accelerating, the power demand is high and so the exhaust flow rate increases and reaches the highest values at high engine speeds and loads. When the vehicle ceases to accelerate the flow rate drops; when the vehicle stops, and during certain braking sections, the engine idles and so the mass flow reach its minimum value. While driving, the concentration of CO_2 in the exhaust line varies from roughly 4% to 9%, and drops to zero when the vehicle is braking. The jagged exhaust flow rate and CO_2 measured with PEMS reflect the gear changes as the mass flow is strongly dependent on the engine speed. The variability of the exhaust flow rate is often also reflected in the CO_2 measurements of the mobile platform, where we can observe similar drops in the CO_2 signal when a gear shift is made (e.g. after 25^{th} to 30^{th} and 160^{th} to 170^{th} seconds, and so on etc.).

The calculated DR values range from approximately 100, when we were in closer proximity to the chased vehicle and the speed of both vehicles was lower; to the maximum value of approximately 72000 when both the emitted CO_2 and the exhaust mass flow rate dropped. This occurred at the end of the track where we had to slow down to make a sharp U-turn. Notwithstanding this period, the maximum DR value was 8943 and the median 1077. This is similar to the measurements of Vogt et al. (2003), where they report dilution factors measured at approximately constant distances of 14, 50 and 100 m distance from a diesel car travelling 50-100 km/h to range from 926 to 9300.

The dilution does not affect the calculated BC EF. As we can see from Figure , the BC EF is at its highest just before the highest cruising speed is reached; and the dilution ratio is highest when the exhaust mass flow rate drops. This is consistent with the findings of Chang et al. (2009), who report that the dilution ratio depends not only on speed but also on the exhaust flow rate and other parameters, which are more important in the near wake region. The omitted parts, when the CO_2 drops below the background, overlap with the parts where there is little to no CO_2 emitted from the exhaust pipe, and so the CO_2 concentrations measured with the mobile station do not exceed the background level. However, the dilution rate does influence the uncertainty of the EF calculation. We can see that both the positive and the negative errors increase at the end of each run when the exhaust mass flow rate drops. We can also see that, at around the 170^{th} second and after the 370^{th} second, there is no positive error. This is because we do not calculate the EF when concentrations drop below the set baseline.

If we had high background noise and low CO_2 emissions coming out of the vehicle, the error produced would have been large. We have, in part, limited calculating with low CO_2 by calculating the running integration EF using the 10 s time integrals instead of shorter intervals.

We will describe the EF variation measured with its range and selected percentile values. The range describes the spread of the sample data. The percentiles divide the sample so that for the pth percentile of a sample (p being a number between 0 and 100), as nearly as possible p% of the sample values are less than the p^{th} percentile and $(100 - p)$% are greater (Navidi, 2001). For each EF time series determined using different background levels, we calculated the distribution range, and the 25^{th}, 50^{th} (median), 75^{th} and 90^{th} percentile values. In Table we can see that the negative relative error is smaller than the positive for values that are the median or higher. We can also see that the maximum value is calculated with the highest uncertainty, but that the 90^{th} percentile uncertainty already resembles the uncertainty of the 75^{th} percentile. This means only a maximum of 10% of the values have an uncertainty that is higher than 25%. We can see that the error that arises from background determination is larger than that arising from instrument imprecision and the omission of CO and HC measurements.

In order to better resolve the EF variability, we have calculated the EF using a shorter integration time of 2 s. In order to calculate the 2 s integration interval we eliminated all values that were lower than the background plus two standard deviations of its variability, thereby excluding low CO_2 values from the calculation, which are the source of the highest EF calculation uncertainty. We can see in Table, that an integration using a shorter time interval of 2 s yields in similar EF distribution values, only the maximum emissions are substantially higher. As Ajtay et al. (2005) reported for their laboratory experiments, the emission peaks flatten on their way from the engine through the exhaust system and the sampling lines of the measuring instruments. During our measurements there is a rapid, intense dilution of exhaust emissions in the atmosphere before they reach the mobile measurement platform. Even by integrating with shorter time interval we can only capture only a smoothened version of the emission peak. Since the uncertainty of such a calculation is rather high, we use the 10 s integration, which thus reflects an even more smoothed version of the super emission peaks produced by the engine.

Table T1. The emission factor (EF) calculated using different background levels shows that regardless of the set background, the EF distributions yield similar percentile values. The + and – signs denote the EF calculated using the background with subtracted 2 standard deviations of its variability (EF BC-), and from the background with added 2 standard deviations of its variability (EF BC+). Their positive and negative relative errors (rel. err.) are also reported. In the last column is the EF is calculated with a 2 s integral instead of a 10 s integral.

	EF BC- (g/kg)	**EF BC (g/kg)**	EF BC+ (g/kg)	-Rel err. (%)	+Rel err. (%)	**EF BC 2 s (g/kg)**
Minimum	0.24	0.23	0.23	-0.04	0.00	0.14
25th percentile	0.50	0.55	0.59	0.09	0.07	0.49
Median	**0.63**	**0.73**	**0.88**	**0.14**	**0.21**	**0.73**
75th percentile	0.85	1.01	1.25	0.16	0.24	1.15
90th percentile	1.17	1.35	1.69	0.13	0.25	1.65
Maximum	1.99	2.44	3.54	0.18	0.45	5.14

Supplementary material S4 – EF figures in linear scale

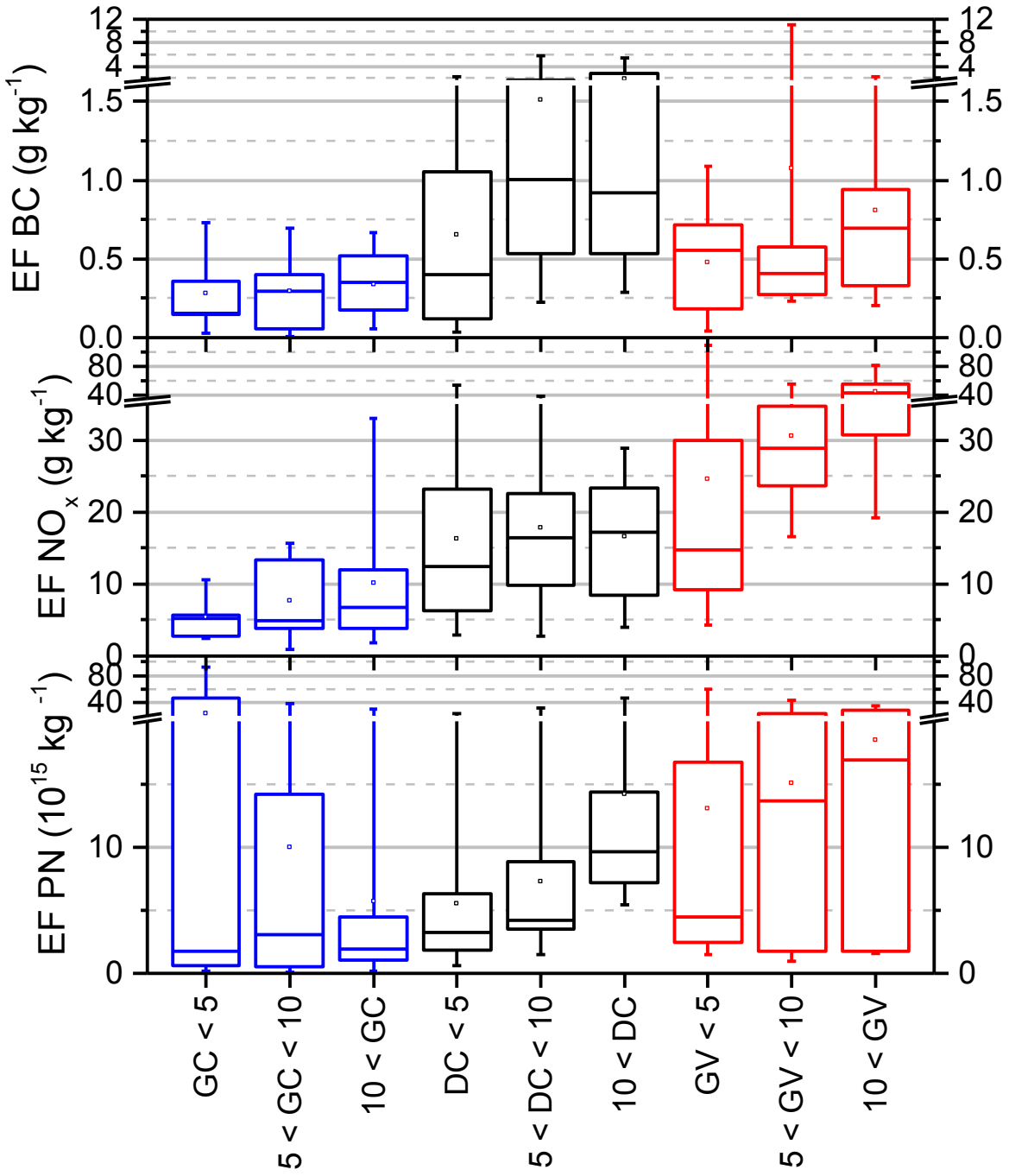

Figure S3. BC and NOx EF according to different vehicle categories and age group subcategories: gasoline passenger cars (GC, blue), diesel passenger cars (DC, black), and goods vehicles (GV, red). Note the EF linear scale; same figure in logarithmic scale can be found as Figure 3.

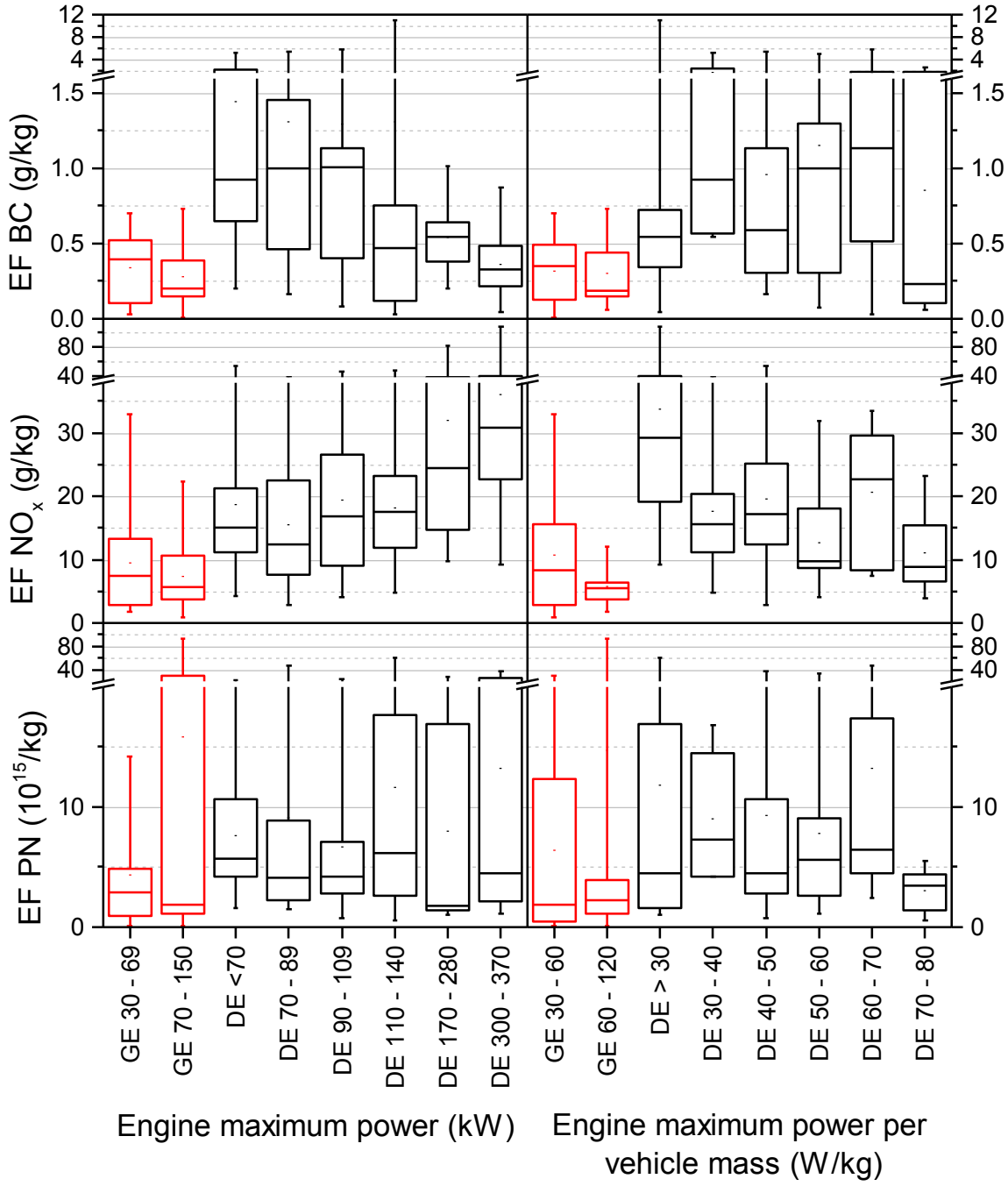

Figure S4. BC and NOx EFs according engine power (left) and size (right); red boxes present gasoline engines (GE) and black boxes present all diesel engines (DE) regardless of their vehicle category. Note the EFs are on logarithmic scale; same figure in logarithmic scale can be found as Figure 4.

References

ACEA: The Automobile Industry Pocket Guide, ACEA Commun. Dep., 2012.

Ajtay D, Weilenmann M and Soltic P.: Towards accurate instantaneous emission models Atmos. Environ., 39 (13), 2443–2449, doi:10.1016/j.atmosenv.2004.03.080, 2005.

Chang V. W. C., Hildemann L. M. and Chang C.: Dilution rates for tailpipe emissions: effects of vehicle shape, tailpipe position, and exhaust velocity, J. Air Waste Manag. Assoc. 59, 715–724, 2009.

Dockery, D. W., Pope, C. A., Xiping, X., Spengler, J. D., Ware, J. H., Fay, M. E., Ferris, B. J. and Speizer, F. E.: An association Between Air Pollution and Mortality in Six U.S. Cities, N. Engl. J. Med., 329, 1759, 1993.

European Parliment: Regulation (EC) No. 715/2007 of the European Parliament and of the Council of 20 June 2007 on type approval of motor vehicles with respect to emissions from light passenger and commercial vehicles (Euro 5 and Euro 6) and on access to vehicle repair and ma, Off. Journal Eur. Union, 171, 1–16, 2007.

Harrison, R.M., Brimblecombe, P., and Derwent, R.G.: Airborne Particulate Matter in the United Kingdom. Third report of the Quality of Urban Air Review Group,Department of the Environment, London, 47, 38-130, 1996.

Heywood, J. B.: Internal Combustion Engine Fundamentals, McGraw-Hill Inc., 1988.

Ježek, I., Drinovec, L., Ferrero, L., Carriero, M. and Močnik, G.: Determination of car on-road black carbon and particle number emission factors and comparison between mobile and stationary measurements, Atmos. Meas. Tech., 8, 43–55, doi:10.5194/amt-8-43-2015, 2015.

Kennedy, I. M.: The health effects of combustion-generated aerosols, Proc. Combust. Inst., 31 II, 2757–2770, doi:10.1016/j.proci.2006.08.116, 2007.

Kittelson, D. B.: Engines and nanoparticles : a review, J. Aerosol Sci., 29(5), 575–588, 1998.

Kittelson, D., Watts, W. and Johnson, J.: On-road and laboratory evaluation of combustion aerosols—Part1: Summary of diesel engine results, J. Aerosol Sci., 37, 913–930, 2006.

Navidi W.: Statistics for engeneers and scientists, vol 40, eds. D B Hash and L Neyens (New York: McGraw-Hill), 2001.

Sharma, M., Kumar, A. and Bharathi, K. V. L.: Characterization of exhaust particulates from diesel engine, Atmos. Environ., 39, 3023–3028, doi:10.1016/j.atmosenv.2004.12.047, 2005.

Tavčar, G., Bizjan, F. and Katrašnik, T.: Methods for improving transient response of diesel engines - influences of different electrically assisted turbocharging topologies, Proc. Inst. Mech. Eng. Part D J. Automob. Eng., 225(9), 1167–1185, doi:10.1177/0954407011414461, 2011.

1 Vogt R., Scheer V., Casati R. and Benter T.: On-road measurement of particle emission in the
2 exhaust plume of a diesel passenger car, Environ. Sci. Technol., 37, 4070–4076, 2003.

3 Xi, J. and Zhong, B.-J.: Soot in Diesel Combustion Systems, Chem. Eng. Technol., 29(6),
4 665–673, doi:10.1002/ceat.200600016, 2006.